

# Microfluidic On-Chip Production of Alginate Hydrogels Using Double Coflow Geometry

Amirmohammad Sattari, Sajjad Janfaza, Mohsen Mashhadi Keshtiban, Nishat Tasnim, Pedram Hanafizadeh,\* and Mina Hoorfar\*



Cite This: *ACS Omega* 2021, 6, 25964–25971



Read Online

ACCESS |



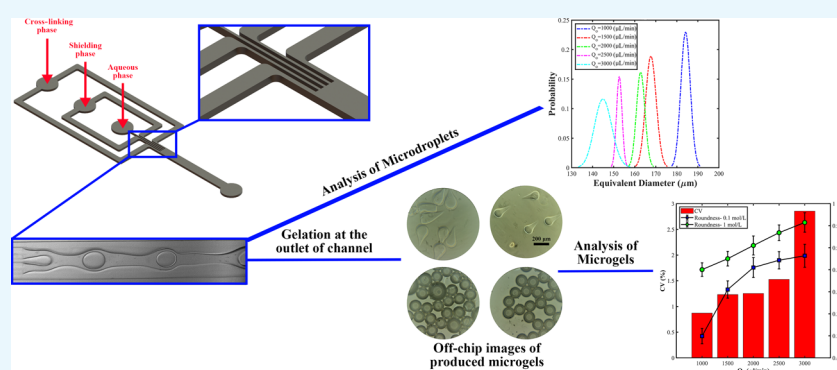
Metrics & More



Article Recommendations



Supporting Information



**ABSTRACT:** Microfluidic on-chip production of microgels employing external gelation has numerous biological and pharmaceutical applications, particularly for the encapsulation of delicate cargos; however, the on-chip production of microgels in microfluidic devices can be challenging due to problems such as clogging caused by accelerated progress in precursor solution viscosity. Here, we introduce a novel microfluidic design incorporating two consecutive coflow geometries for microfluidic droplet generation. A shielding oil phase is employed to avoid emulsification and gelation stages from occurring simultaneously, thereby preventing clogging. The results revealed that the microfluidic device could generate highly monodispersed spherical droplets (coefficient of variation < 3%) with an average diameter in the range of 60–200  $\mu\text{m}$ . Additionally, it was demonstrated that the device could appropriately create a shelter of the oil phase around the inner aqueous phase regardless of the droplet formation regime and flow conditions. The ability of the proposed microfluidic device in the generation of microgels was validated by producing alginate microgels utilizing an aqueous solution of calcium chloride as the continuous phase.

## INTRODUCTION

There has been a thriving interest in microfluidics due to their breadth of applications in diverse branches of science and industry, from biological applications to food science and chemistry. By operating at a miniature scale, microfluidic systems can offer advantages such as regulating and manipulating fluids with tremendous precision, enabling precise control over small sample volumes, and reducing analysis time.<sup>1</sup> Attention to the droplet-based microfluidic systems has been expanding extensively in past decades due to their substantial applications in various areas, such as cell culture,<sup>2</sup> chemical synthesis,<sup>3</sup> and extraction and phase transfer.<sup>4</sup>

The production of emulsions and microparticles employing microfluidic platforms has gained noteworthy attention in recent years due to their significant benefits over traditional bulk methods.<sup>5</sup> In the so-called bulk methods, such as precipitation polymerization and emulsion polymerization, there is minimal control over particle monodispersity, uniformity of cross-link density, and morphology, especially

for creating complex geometries such as multiple emulsions.<sup>6</sup> In contrast, droplet-based microfluidics systems facilitate practical and precise control in the fabrication of microparticles and emulsions.<sup>7</sup> Monodispersed microdroplets generated in microfluidic platforms can provide a compartment in which reactions or species can be separated from the surrounding environment, so it is fitting for quantitative investigations on cell analysis applications and suggests a meaningful number of opportunities in biological and chemical applications.<sup>8</sup> Furthermore, the droplet-based microfluidics technology allows the generation of monodispersed and shape-controlled microgels, which has numerous applications in cell biology,<sup>9</sup>

Received: May 25, 2021

Accepted: September 15, 2021

Published: September 30, 2021



tissue engineering,<sup>10</sup> drug delivery,<sup>11</sup> and separation processes.<sup>12</sup>

The microfluidic production of the microgels typically consists of two steps, including microfluidic emulsification of forerunner solutions and gelation of the produced droplets, which can be done in either on-chip or off-chip mode. The on-chip gelation method is commonly favored since it has numerous advantages over off-chip gelation, including simplified manipulation of the microgels' morphologies, facilitated way for loading a wide diversity of cargos, and continuous production of the microgels with an extraordinary degree of monodispersity.<sup>13,14</sup> Yet, there are several outstanding challenges with the on-chip gelation method, one major factor being the immediate development of the cross-linking process, which may result in the occlusion of the microchannels and/or inlets and outlets. The production of microgel with controlled morphology and dispersity also requires the inclusion of a time lag between the emulsification and gelation processes.<sup>14</sup> Several research groups have come up with some innovative ideas to solve this issue. One novel idea, first proposed by Wang et al.,<sup>15</sup> took advantage of a blocking stream to prevent premature gelation. In their study, a water stream was incorporated in the middle microchannel to inhibit the mixing of ionic triblock copolymers with a separate charge, which moves in the side microchannels prior to the flow-focusing nozzle. Similar work was presented by Mazutis et al.,<sup>16</sup> employing a two-consecutive flow-focusing configuration. They passed a water flow stream from the central channel, which prevented the immature generation of alginate microgels from cross-linking with the calcium chloride solution. The proposed methods are relatively effective but have some limitations, including challenging chemical processes and the complicated microfabrication processes of the microfluidic devices.

Microfluidic preparation of precursor solutions can be fundamentally classified into two approaches: channel-based microfluidics and planar surface approach.<sup>17</sup> In the so-called channel-based systems, the interaction among continuous and dispersed phases causes the breakup and generation of single droplets. In contrast, in the planar surface technique, or as regularly called digital microfluidics, from an actuation mechanism through electrowetting or dielectrophoresis techniques, the breakup occurs.<sup>18</sup> There are some conventional geometries to generate droplets in microfluidic systems, namely, T-junction,<sup>19</sup> flow-focusing,<sup>20</sup> coflowing,<sup>21</sup> membrane,<sup>22</sup> and step emulsification,<sup>23</sup> which are classified in channel-based microfluidics. As a general comparison between mentioned emulsification methods, membrane structures provide the highest throughput while they suffer from a relatively poor monodispersity.<sup>24</sup> From another point of view, among the mentioned structures, coflow geometry requires a minimum surface treatment procedure because the core fluid stream remains enclosed within the continuous stream during droplet formation.<sup>25</sup> Hence, the inner jet stream does not touch the microchannel wall, and therefore no surface wall treatment is required for the production of microdroplets. This configuration also benefits from high monodispersity and significant throughput of droplet generation compared to other conventional geometries.<sup>1</sup> Various combinations of the aforementioned geometries have been widely used, taking advantage of both geometry<sup>26</sup> and generation of double emulsions<sup>27</sup> such as two subsequent T-junctions,<sup>28</sup> flow-focusing,<sup>29</sup> coflowing,<sup>30</sup> a combination of T-junction and

coflowing,<sup>31</sup> and a combination of T-junction and flow-focusing.<sup>32</sup> As discussed earlier, on-chip gelation of microdroplets still remained a challenging technique due to the need to precisely control the gelation process within the microchannel, which requires to be studied more.

As discussed before, the on-chip gelation process is generally preferred because it has several benefits over off-chip gelation. Therefore, many studies have been performed in the area of on-chip gelation. However, they suffer from complicated chemical processes and/or complex microfabrication processes (such as step emulsification). Hence, a novel microfluidic approach for the on-chip production of microgels is necessary, which has both high control over the production of highly monodispersed and spherical microgels and also easy fabrication of the microfluidic device to make it feasible in various applications. Also, the use of a double geometry can significantly improve the efficiency of on-chip gelation by taking advantage of a shielding phase and delaying the cross-linking process up to the end of the microfluidic device. It is clear that the single geometry only handles the inner alginate phase and the cross-linking phase, which can arise the problem of clogging the microfluidic chip due to the cross-linking in the microfluidic device.

To obtain monodispersed microgels, several strategies have been introduced in the literature, such as the use of a high concentration of surfactants in W/O microfluidic devices. However, these methods have limitations in some biological applications such as cell and enzyme encapsulation. For instance, high concentrations of surfactants are toxic to the cells and affect the functionality of proteins and enzymes.<sup>33</sup>

In this study, we developed a novel and simply fabricated microfluidic device for the generation of highly monodispersed spherical microgels using double coflow geometry. Our proposed design included the features of facile emulsification and controllable gelation to mitigate challenges associated with the microfluidic production of microgels. Regarding the emulsification process, we employ a double coflow geometry composed of the two same-level high-aspect-ratio coflow channels introduced in our previous study (Sattari & Hanafizadeh, 2020). In the proposed double coflow geometry, a shielding oil phase is used to cover the forming jet of the inner phase right at the beginning of its formation. This results in extending the cross-linking process up to the end of the microchannel, creating highly monodispersed and spherical droplets. We have also examined the effects of all three phase flow rates on the diameter and size distribution of microdroplets. Besides, an off-chip evaluation of the shape and size of microgels revealed a successful gelation process in the proposed microfluidic device.

## ■ MATERIALS AND METHODS

**Materials.** The inner phase consisted of 1.5% (wt) of sodium alginate (19–40 kDa) dispersed in deionized water. The shielding phase consisted of a mixture of 0.3% (w/w) of Span 80 in light mineral oil (Sigma-Aldrich). The cross-linking phase comprised an emulsion of calcium chloride aqueous solution as a cross-linking agent with two different concentrations of 0.1 and 1 mol/L. All experiments were conducted at room temperature (20 °C) and atmospheric conditions (1 bar).

**Geometric Model.** The proposed geometry comprises three distinct rectangular microchannels with the same axis, which is shown in Figure 1a. All three internal channels have a

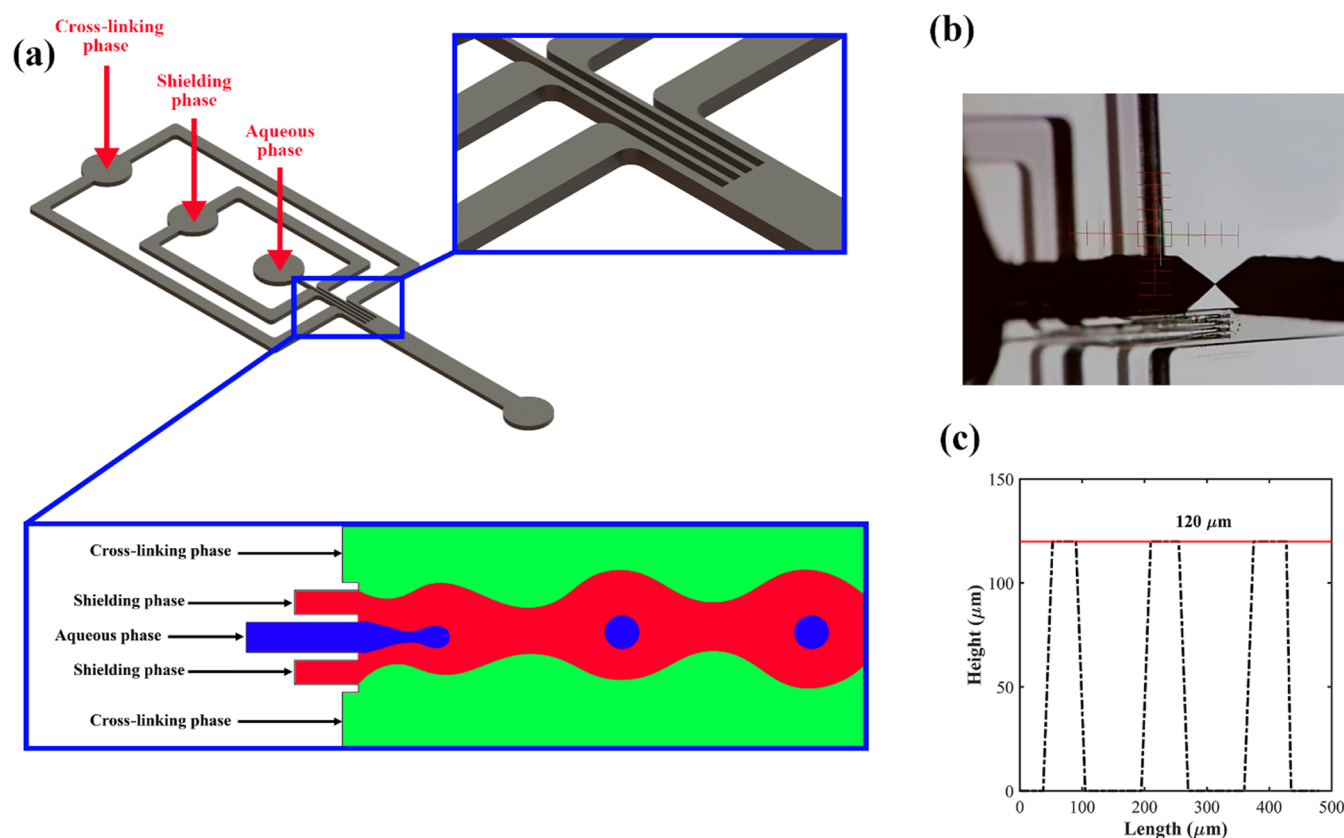


**Figure 1.** (a) Three-dimensional view of the designed double coflow geometry, (b) an image of the surface profilometer device, and (c) results of the profile obtained from the surface profilometry.

width of  $40\ \mu\text{m}$ , while the outer channels close to the side walls have a  $60\ \mu\text{m}$  width, and the microfluidic chip has a constant height of  $120\ \mu\text{m}$ . The inner phase is introduced through the central channel, while the intermediate shielding phase is injected from its two side channels. The cross-linking phase also flows from the outermost channels. The total length of the main channel is about  $5000\ \mu\text{m}$ , which is sufficient for diminishing the effects of the outlet on the droplet formation. All inlets and outlets are circular in shape with an average diameter of  $1100\ \mu\text{m}$ .

The shape of the fabricated mold, particularly at the junctions, was assessed with the use of a surface profilometer (Profil3D, Filmetrics). A view of the probe passing along the fabricated mold is presented in Figure 1b. The profile of the silicone-SU-8 mold showed a satisfactory depth and proper space between walls (Figure 1c).

**Microfabrication.** The polydimethylsiloxane (PDMS) channel was produced in the cleanroom using an SU-8 mold fabricated on a silicon substrate. SU-8 2075 (MicroChem Corp) was spin-coated on a 3 inches silicon wafer considering the guideline provided by MicroChem to achieve a  $120\ \mu\text{m}$  mold height. The silicon wafer was soft-baked at  $65$  and  $95\ ^\circ\text{C}$  for 3 and 5 min, respectively. It was then exposed to ultraviolet (UV) light and proceeds under postexposure bake (PEB) at  $95\ ^\circ\text{C}$  for 5 min. Instantly, the silicon wafer was immersed in the SU-8 developer for about 8 min and patterned. After wiping with isopropanol, the mold was hard-baked for almost 30 min at  $150\ ^\circ\text{C}$ .

A proper amount of PDMS and its curing agent (Dow Corning) are mixed with a 10:1 ratio and poured over the mold. Following the elimination of bubbles in a desiccator and

curing in the oven at  $70\ ^\circ\text{C}$  for about 5 hours, the PDMS channel was peeled off, and the inlets and outlets were punched using a 1 mm puncher. Ultimately, the PDMS and glass surfaces are treated in an oxygen plasma chamber and are bonded immediately.

**On-Chip Gelation.** To generate alginate microgels, the inner aqueous phase containing 1.5% w/w of alginate in deionized (DI) water was inserted from the central channel and the shelter phase containing 0.3% w/w of Span 80 in light mineral oil was injected through the side channels. The mineral oil acted as the continuous phase for the generation of alginate microdroplets, as well as a shelter phase to prevent the immediate development of the cross-linking process. The cross-linking phase consisted of an aqueous solution of calcium chloride with two various concentrations of  $0.1$  and  $1\ \text{mol L}^{-1}$ , which was flowed through the outermost channels.

In the proposed configuration, alginate microdroplets remained enclosed by the shelter phase up to the end of the main channel. At the outlet, which functioned as a step due to a greater height compared to the other parts of the microchannel, the shelter phase ruptured, resulting in the penetration of the cross-linking phase to the alginate microdroplets, creating microgels at the outlet of the device. The produced microgels then left the device through a silicone tube and were collected in microtubes. It should be noted that using the proper concentration of calcium chloride in the cross-linking phase (more than  $1\ \text{mol L}^{-1}$ ) leads to highly monodispersed and spherical droplets due to the prevention from the cross-linking process through the channel and gelation process right at the outlet.

**Experimental Setup and Image Analysis.** The setup includes a biological microscope (Zeiss Company, Germany), a high-speed video camera (XIMEA Company, Germany), three automatic syringe pumps (SAMA Instruments) for relatively constant flow infusion to the microfluidic channels, the microfabricated PDMS chip, a computer for collecting videos and controlling the syringe pumps, and a reservoir for collecting generated microgels. Videos were obtained at a frequency rate of 2000 Hz and were analyzed using droplet morphometry and velocimetry (DMV) Matlab-based software.<sup>34</sup>

## RESULTS AND DISCUSSION

We have investigated the influence of phase flow rates on the overall diameter and size distribution of microdroplets in dual coflow geometry, with the presence of shielding oil phase. Also, we have studied the effects of the outer phase flow rate and calcium chloride concentration on the roundness and size distribution of produced microgels.

**Overall Observation.** The formation of alginate droplets shielding by the middle oil phase from the continuous cross-linking phase in various flow conditions is depicted in Figure 2.

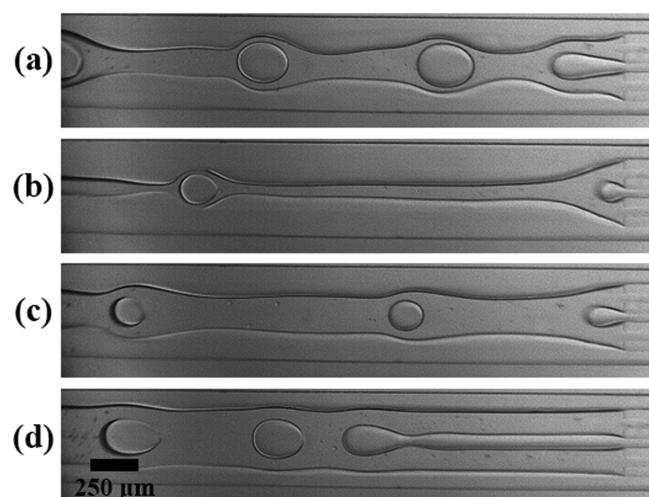


**Figure 2.** Shielding of alginate droplets by shelter oil phase in (a)  $Q_i = 0.5 \mu\text{L}/\text{min}$ ,  $Q_m = 1 \mu\text{L}/\text{min}$ ,  $Q_o = 1000 \mu\text{L}/\text{min}$ ; (b)  $Q_i = 0.5 \mu\text{L}/\text{min}$ ,  $Q_m = 1 \mu\text{L}/\text{min}$ ,  $Q_o = 3000 \mu\text{L}/\text{min}$ ; (c)  $Q_i = 0.5 \mu\text{L}/\text{min}$ ,  $Q_m = 100 \mu\text{L}/\text{min}$ ,  $Q_o = 1000 \mu\text{L}/\text{min}$ ; and (d)  $Q_i = 10 \mu\text{L}/\text{min}$ ,  $Q_m = 1 \mu\text{L}/\text{min}$ ,  $Q_o = 1000 \mu\text{L}/\text{min}$ .

In all flow conditions, the middle oil phase prevents the inner alginate droplets from cross-linking with the continuous phase along the microchannel. At the end of the main channel, the middle oil phase ruptures, and the cross-linking process begins. Note that because of the presence of the silicone tube at the outlet of the channel, the direct observation of the mentioned happenings was not possible. Nevertheless, the off-chip observation of cross-linked alginate droplets showed the commencement of cross-linking at the outlet of the designed microchip. For a better understanding of the procedure of droplet formation, a supplementary video corresponding to Figure 2a is provided in the Supporting Information (SI 1).

As a general observation, increasing the continuous phase flow rate results in smaller alginate droplets and a narrower shielding phase jet (Figure 2a,b). Similarly, an increment in the flow rate of the middle phase leads to the smaller alginate

droplets due to the higher shear rate imposed by the middle oil phase. However, the higher momentum of the shielding jet overcomes the shear rate acted upon by the cross-linking phase to its interface and results in a wider shielding jet stream (Figure 2a,c). Finally, the inner phase flow rate growth results in the transition from dripping to the jetting regime. This leads to both larger droplets and wider middle phase jet stream because the shielding jet is blocked by the forming jet of the inner alginate stream (Figure 2a,d).

**Effect of Outer Phase Flow Rate.** The influence of cross-linking phase flow rate on the alginate droplets' equivalent diameter and size distribution is demonstrated in Figure 3. As seen in the figure, the increment of the continuous phase flow rate resulted in smaller alginate droplets. The decrease in the inner droplet diameter is principally due to increased shear stress implemented by the continuous phase stream to the shielding phase jet interface. Increasing the outer phase velocity manages the suppression of the oil phase jet, which also diminishes the formation time and tends to the formation of smaller alginate droplets.

Of note, higher cross-linking phase flow rates lead to the higher polydispersity of the size of alginate droplets, i.e., the coefficient of variation is larger in the condition of the higher shear rate imposed to the forming jet of the inner phase. This can be justified by the fact that the higher shear rates imposed by the continuous phase result in the shielding phase jet stream moving away from a symmetrical shape due to the higher instabilities on the shielding jet interface. This creates a disturbance in the formation of alginate droplets leading to the lower monodispersity of droplets.

**Effect of Shielding Phase Flow Rate.** The effects of middle phase flow rate on the alginate droplets' equivalent diameter and size distribution are demonstrated in Figure 4. As shown, the increment of the shielding phase flow rate results in smaller alginate droplets and transitions from jetting to dripping regimes. Also, the middle phase jet gets wider whatever the middle phase flow rate increases, and also fewer numbers of instabilities can be seen. The decrease in the inner droplet diameter is essentially due to the larger shear stress implemented by the oil phase stream to the inner droplet interface. Thus, it manages the suppression of the alginate phase jet, leading it to the dripping regime and causing the formation of smaller droplets. Furthermore, the size distribution of microdroplets is much narrower in the dripping regime (higher flow rates of middle oil phase), and therefore alginate droplets had higher monodispersity than in lower flow rates of the middle phase and jetting regime.

**Effect of Alginate Phase Flow Rate.** The increment of the inner phase flow rate led to the transition from the dripping to the jetting regimes and also the formation of larger alginate droplets, as shown in Figure 5. An increase in the innermost phase velocity leads to a growth in the inner phase droplet diameter. The growth in droplet diameter occurs as a result of the increase in both inertial and viscous forces of the internal phase, which indicates that more surface tension force is expected to dominate inertia and viscous forces for the breakup process that is achieved by larger droplets in constant surface tension states. Furthermore, due to the transition from dripping to the jetting regime at higher inner phase flow rates, the monodispersity diminishes as the inner phase flow rate increases.

**Off-Chip Investigation of Alginate Microgels.** We have also investigated the effect of calcium chloride concentration in

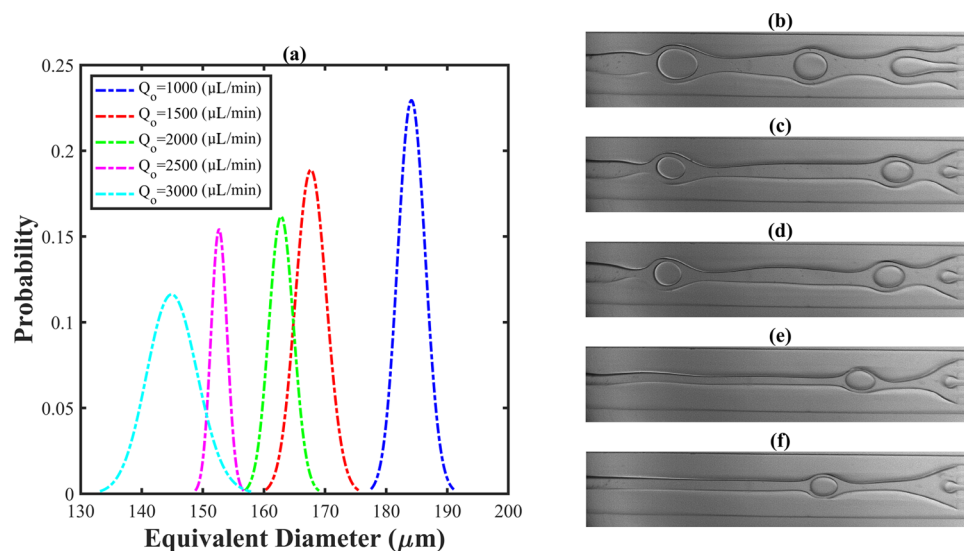


**Figure 3.** (a) Probability of droplet diameter as a function of the outer phase flow rate. Shielding of alginate droplets by shelter oil phase in (b)  $Q_o = 1000 \mu\text{L}/\text{min}$ , (c)  $Q_o = 1500 \mu\text{L}/\text{min}$ , (d)  $Q_o = 2000 \mu\text{L}/\text{min}$ , (e)  $Q_o = 2500 \mu\text{L}/\text{min}$ , and (f)  $Q_o = 3000 \mu\text{L}/\text{min}$ . Inner and middle phase flow rates are kept constant and equal to  $Q_i = 0.5 \mu\text{L}/\text{min}$  and  $Q_m = 1 \mu\text{L}/\text{min}$ .

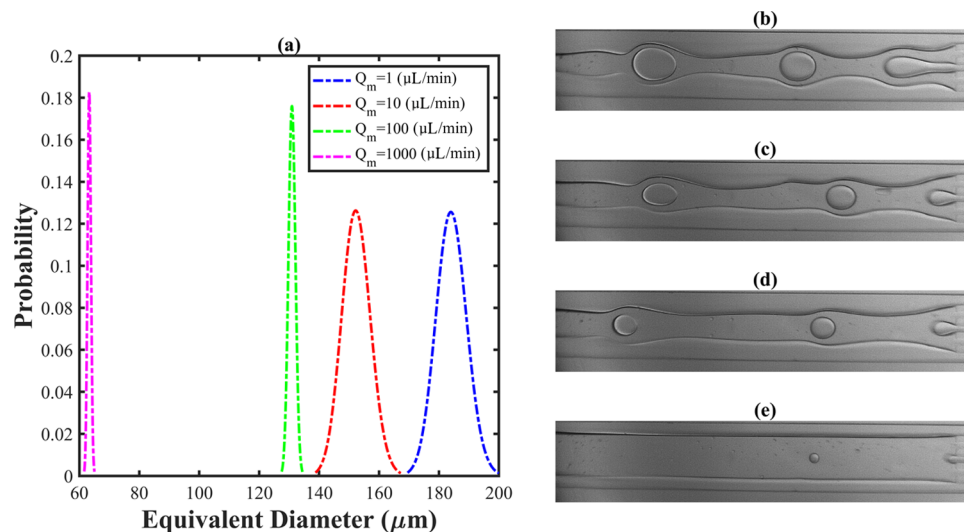


**Figure 4.** (a) Probability of droplet diameter as a function of the middle phase flow rate. Shielding of alginate droplets by shelter oil phase in (b)  $Q_m = 1 \mu\text{L}/\text{min}$ , (c)  $Q_m = 10 \mu\text{L}/\text{min}$ , (d)  $Q_m = 100 \mu\text{L}/\text{min}$ , and (e)  $Q_m = 1000 \mu\text{L}/\text{min}$ . Inner and outer phase flow rates are kept constant and equal to  $Q_i = 0.5 \mu\text{L}/\text{min}$  and  $Q_o = 1000 \mu\text{L}/\text{min}$ .

the cross-linking phase emulsion on the capability of synthesis of microgels. To analyze this parameter, the concentrations of calcium chloride were considered as 0.1 and 1 mol/L. In low calcium chloride concentrations, nonspherical microgels with a drop-like shape (also called the teardrop or tail-shaped) were produced (Figure 6a,b). The production of teardrop-shaped microgels indicated that complete gelation process or most of it occurred outside of the microfluidic device in the outlet tube.<sup>14,35</sup> An observation that verifies this theory is the formation of spherical alginate droplets during our experiments. As shown in Figure 2, the generated alginate droplets were quite spherical, and if their gelation process occurred solely in the microfluidic device, the produced microgels should be spherical as well. Even if the gelation process occurs partly (just a shell forms around the alginate droplets), provided that this shell has a sufficient thickness, it can sustain

the spherical shape of microgels after leaving the microfluidic chip.<sup>36</sup>

As represented in Figure 6c,d, the shape of the produced microgels became more spherical by increasing calcium chloride concentrations. This observation confirms that at higher concentrations of calcium chloride, a greater portion of the gelation process occurs inside the microfluidic device, and consequently, microgel production shifts to a more on-chip process. This remark is presumably due to the quicker diffusion of more calcium ions from the cross-linking phase into the alginate droplets at higher calcium chloride concentrations. Thus, this will cause faster gelation of alginate droplets, leading to on-chip gelation of these droplets and sustaining their spherical shape after gelation.

We examined the influence of the outer phase flow rate on the gelation process, as depicted in Figure 6. As discussed previously, the increment in the external phase flow rate leads

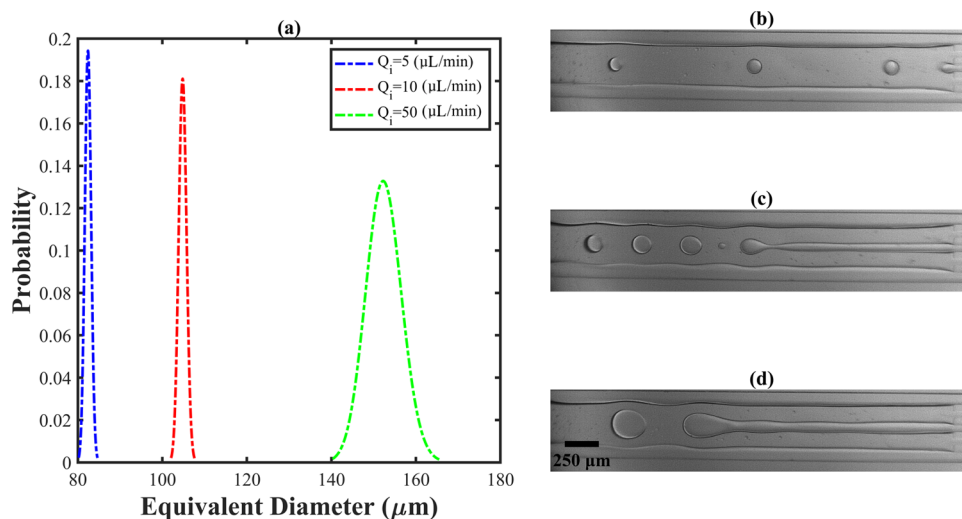


**Figure 5.** (a) Probability of droplet diameter as a function of the inner phase flow rate. Shielding of alginate droplets by shelter oil phase in (b)  $Q_i = 5$   $\mu\text{L}/\text{min}$ , (c)  $Q_i = 10$   $\mu\text{L}/\text{min}$ , and (d)  $Q_i = 50$   $\mu\text{L}/\text{min}$ . Middle and outer phase flow rates are kept constant and equal to  $Q_m = 10$   $\mu\text{L}/\text{min}$  and  $Q_o = 1000$   $\mu\text{L}/\text{min}$ .

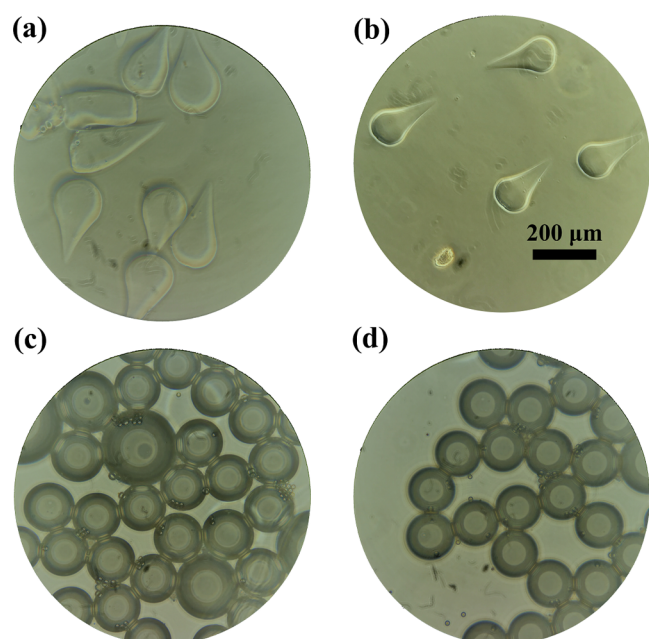


**Figure 6.** Alginate microgels were synthesized using the proposed double coflow microfluidic device. Calcium chloride concentrations in the cross-linking phase are 0.1 mol/L (a, b) and 1 mol/L (c, d). The formation of cross-linked alginate droplets in (a, c)  $Q_o = 1000$   $\mu\text{L}/\text{min}$  and (b, d)  $Q_o = 2000$   $\mu\text{L}/\text{min}$ . Inner and middle phase flow rates are kept constant and equal to  $Q_i = 0.5$   $\mu\text{L}/\text{min}$  and  $Q_m = 1$   $\mu\text{L}/\text{min}$ .

to the smaller alginate droplets. Consequently, smaller cross-linked droplets can be seen in both concentrations (Figure 6b,d) compared to Figure 6a,c). We observed that the roundness of the droplets' shape was slightly greater in higher flow rates of the outer phase than that in the lower flow rates. This indicated that a more significant portion of the gelation process occurred inside the microfluidic device, and microgel generation shifts to an on-chip process. That was predictable since the cross-linking phase flow rate increment leads to a narrower intermediate shielding phase; consequently, the penetration of the cross-linking phase into the alginate microdroplets is more readily compared to the broader middle

phase jet stream conditions, and most of the gelation process occurred on-chip.

It should be noted that the most important evidence of cross-linking is solidification of the alginate that makes microbeads stable. As Figure 6 shows, the microgels are very stable and do not collapse or merge to gather, which is due to the fully cross-linking of the alginate microgels.

#### Effect of Outer Phase Flow Rate and Calcium Chloride Concentration on Characteristics of Microgels.

The quantitative measurement of roundness and coefficient of variation in various outer phase flow rates and two distinct concentrations of calcium chloride was performed and is shown in Figure 7. The increment in the outer phase flow rate leads to the lower monodispersed droplets, i.e., a higher coefficient of variation. The decrease in monodispersity can be

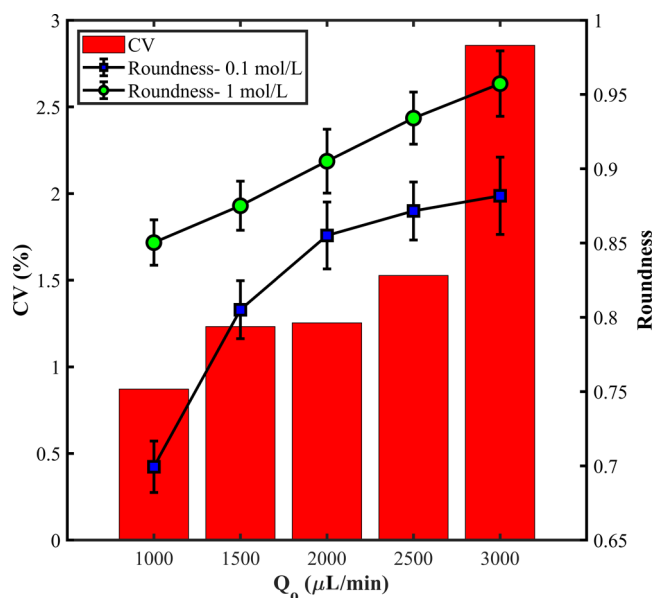


**Figure 7.** Effect of continuous phase flow rate and calcium chloride concentration on the coefficient of variation and roundness of alginate microgels.

attributed to higher shear rates in the continuous phase resulting in a more asymmetrical shape of the shielding phase. Consequently, more disturbances affect the formation of alginate microdroplets, resulting in the lower monodispersity of droplets. Nevertheless, the coefficient of variation of droplet sizes remained under 3% for the worst condition (the highest flow rate of the cross-linking phase), which shows the capability of our proposed device to generate highly monodispersed droplets.

Besides, higher flow rates of the cross-linking phase result in more spherical alginate microgels, and this sphericity enhances more as the concentration of the calcium chloride increases in the cross-linking phase. Generally speaking, the roundness of alginate droplets is not acceptable in low concentrations of calcium chloride at low flow rates of the cross-linking phase ( $Q_o < 2000 \mu\text{L/h}$ ). In contrast, the roundness is quite acceptable in all conditions of the cross-linking phase flow rate for a 1 mol/L calcium chloride concentration (roundness is more than 0.85 in all situations).

As discussed earlier, the roundness is increased by increasing the flow rate of the outer phase. The more the immediate cross-linking at the outlet of the microchannel, the more the roundness of the microgels. In fact, the higher shear rates imposed by the outer phase result in the more facile rupture of the intermediate shielding phase and the beginning of the gelation process right at the end of the microfluidic device. However, the influence of the outer phase flow rate is relatively small, i.e., for the 1 mol/L of the calcium chloride concentration, the roundness only varies 10% as the flow rate increases from 1000 to 3000  $\mu\text{L/min}$ .

## CONCLUSIONS

In this study, the microfluidic on-chip generation of alginate microgels using an external gelation method was accomplished by employing a double coflow configuration. A sheltered oil phase was utilized for alginate droplet shielding, which prevents the process of emulsification and gelation from taking place simultaneously. The effects of phase flow rates on the droplet characteristics, including equivalent diameter and coefficient of variation, were examined. The ability of the proposed device to produce highly monodispersed spherical microgels was confirmed by creating alginate microgels through external gelation of alginate droplets shielded by the mineral oil phase with the calcium chloride continuous phase at the outlet of the device. Moreover, the impact of calcium chloride concentration in the cross-linking phase on the gelation process was investigated. Overall, the experiment results confirmed the ability of double coflow geometry in the production of highly monodispersed spherical microgels. The proposed design is particularly applicable for microfluidic encapsulation of sensitive loads using microgels due to the adopted shielding phenomenon and on-chip external gelation method. The proposed technology can be employed for microencapsulation of a variety of biomolecules and cells for different purposes such as protecting them from the harsh environment. Such research will be the subject of our future studies.

## ASSOCIATED CONTENT

### Supporting Information

The Supporting Information is available free of charge at <https://pubs.acs.org/doi/10.1021/acsomega.1c02728>.

Process of droplet formation in a double coflow device in the presence of the shielding phase; the operating conditions are  $Q_i = 0.5 \mu\text{L/min}$ ,  $Q_o = 1 \mu\text{L/min}$ , and  $Q_c = 1000 \mu\text{L/min}$  (SI 1) (MP4)

## AUTHOR INFORMATION

### Corresponding Authors

**Pedram Hanafizadeh** – School of Mechanical Engineering, College of Engineering, University of Tehran, Tehran 16589-53571, Iran; Department of Mechanical Engineering, University of California, Berkeley, California 94720, United States; Email: [hanafizadeh@ut.ac.ir](mailto:hanafizadeh@ut.ac.ir)

**Mina Hoorfar** – Department of Mechanical Engineering, University of Victoria, Victoria, BC V8W 3P6, Canada; [orcid.org/0000-0002-2665-7532](https://orcid.org/0000-0002-2665-7532); Email: [mina.hoorfar@ubc.ca](mailto:mina.hoorfar@ubc.ca)

### Authors

**Amirmohammad Sattari** – School of Mechanical Engineering, College of Engineering, University of Tehran, Tehran 16589-53571, Iran; School of Engineering, University of British Columbia, Kelowna, BC V1V 1V7, Canada

**Sajjad Janfaza** – School of Engineering, University of British Columbia, Kelowna, BC V1V 1V7, Canada; Department of Biological Sciences, University of Alberta, Edmonton, AB T6G 2E9, Canada

**Mohsen Mashhadi Keshtiban** – School of Mechanical Engineering, College of Engineering, University of Tehran, Tehran 16589-53571, Iran

**Nishat Tasnim** – School of Engineering, University of British Columbia, Kelowna, BC V1V 1V7, Canada

Complete contact information is available at: <https://pubs.acs.org/doi/10.1021/acsomega.1c02728>

### Author Contributions

A.S.: conceptualization, data curation, formal analysis, investigation, methodology, and writing (original draft); S.J.: data curation, investigation, and methodology; M.M.K.: data curation, formal analysis, methodology, validation, and writing (review and editing); N.T.: writing (review and editing), methodology, and formal analysis; P.H.: conceptualization, investigation, project administration, supervision, and writing (review and editing); and M.H.: conceptualization, investigation, project administration, supervision, and writing (review and editing).

### Notes

The authors declare no competing financial interest.

## ACKNOWLEDGMENTS

This research received no specific grant from any funding agency in the public, commercial, or not-for-profit sectors.

## REFERENCES

- (1) Sattari, A.; Hanafizadeh, P.; Hoorfar, M. Multiphase Flow in Microfluidics: From Droplets and Bubbles to the Encapsulated Structures. *Adv. Colloid Interface Sci.* **2020**, *282*, 102208.
- (2) Joensson, H. N.; Andersson Svahn, H. Droplet Microfluidics—A Tool for Single-cell Analysis. *Angew. Chem., Int. Ed.* **2012**, *51*, 12176–12192.
- (3) Elvira, K. S.; i Solvas, X. C.; Wootton, R. C. R.; Demello, A. J. The Past, Present and Potential for Microfluidic Reactor Technology in Chemical Synthesis. *Nat. Chem.* **2013**, *5*, 905.

- (4) Poulsen, C. E.; Wootton, R. C. R.; Wolff, A.; deMello, A. J.; Elvira, K. S. A Microfluidic Platform for the Rapid Determination of Distribution Coefficients by Gravity-Assisted Droplet-Based Liquid–Liquid Extraction. *Anal. Chem.* **2015**, *87*, 6265–6270.
- (5) Teh, S. Y.; Lin, R.; Hung, L. H.; Lee, A. P. Droplet Microfluidics. *Lab Chip* **2008**, *8*, 198–220.
- (6) Li, W.; Zhang, L.; Ge, X.; Xu, B.; Zhang, W.; Qu, L.; Choi, C. H.; Xu, J.; Zhang, A.; Lee, H.; Weitz, D. A. Microfluidic Fabrication of Microparticles for Biomedical Applications. *Chem. Soc. Rev.* **2018**, *47*, 5646–5683.
- (7) Seemann, R.; Brinkmann, M.; Pfohl, T.; Herminghaus, S. Droplet Based Microfluidics. *Rep. Prog. Phys.* **2012**, *75*, 016601.
- (8) Theberge, A. B.; Courtois, F.; Schaerli, Y.; Fischlechner, M.; Abell, C.; Hollfelder, F.; Huck, W. T. S. Microdroplets in Microfluidics: An Evolving Platform for Discoveries in Chemistry and Biology. *Angew. Chem., Int. Ed.* **2010**, *49*, 5846.
- (9) Girardo, S.; Träber, N.; Wagner, K.; Cojoc, G.; Herold, C.; Goswami, R.; Schlüßler, R.; Abuhattum, S.; Taubenberger, A.; Reichel, F.; Mokbel, D.; Herbig, M.; Schürmann, M.; Müller, P.; Heida, T.; Jacobi, A.; Ulbricht, E.; Thiele, J.; Werner, C.; Guck, J. Standardized Microgel Beads as Elastic Cell Mechanical Probes. *J. Mater. Chem. B* **2018**, *6*, 6245.
- (10) Guermani, E.; Shaki, H.; Mohanty, S.; Mehrali, M.; Arpanaei, A.; Gaharwar, A. K.; Dolatshahi-Pirouz, A. Engineering Complex Tissue-like Microgel Arrays for Evaluating Stem Cell Differentiation. *Sci. Rep.* **2016**, *6*, No. 30445.
- (11) Zhao, C. X. Multiphase Flow Microfluidics for the Production of Single or Multiple Emulsions for Drug Delivery. *Adv. Drug Delivery Rev.* **2013**, *65*, 1420–1446.
- (12) Dendukuri, D.; Doyle, P. S. The Synthesis and Assembly of Polymeric Microparticles Using Microfluidics. *Adv. Mater.* **2009**, *21*, 4071.
- (13) Tumarkin, E.; Kumacheva, E. Microfluidic Generation of Microgels from Synthetic and Natural Polymers. *Chem. Soc. Rev.* **2009**, *38*, 2161–2168.
- (14) Shieh, H.; Saadatmand, M.; Eskandari, M.; Bastani, D. Microfluidic On-Chip Production of Microgels Using Combined Geometries. *Sci. Rep.* **2021**, *11*, No. 1565.
- (15) Wang, C. X.; Utech, S.; Gopez, J. D.; Mabesoone, M. F. J.; Hawker, C. J.; Klinger, D. Non-Covalent Microgel Particles Containing Functional Payloads: Coacervation of PEG-Based Triblocks via Microfluidics. *ACS Appl. Mater. Interfaces* **2016**, *8*, 16914.
- (16) Mazutis, L.; Vasiliauskas, R.; Weitz, D. A. Microfluidic Production of Alginate Hydrogel Particles for Antibody Encapsulation and Release. *Macromol. Biosci.* **2015**, *15*, 1641.
- (17) Mashaghi, S.; Abbaspourrad, A.; Weitz, D. A.; van Oijen, A. M. Droplet Microfluidics: A Tool for Biology, Chemistry and Nanotechnology. *TrAC, Trends Anal. Chem.* **2016**, *82*, 118–125.
- (18) Haeberle, S.; Zengerle, R. Microfluidic Platforms for Lab-on-a-Chip Applications. *Lab Chip* **2007**, *7*, 1094–1110.
- (19) Fu, T.; Ma, Y.; Funfschilling, D.; Zhu, C.; Li, H. Z. Squeezing-to-Dripping Transition for Bubble Formation in a Microfluidic T-Junction. *Chem. Eng. Sci.* **2010**, *65*, 3739–3748.
- (20) Anna, S. L.; Bontoux, N.; Stone, H. A. Formation of Dispersions Using “Flow Focusing” in Microchannels. *Appl. Phys. Lett.* **2003**, *82*, 364–366.
- (21) Utada, A. S.; Fernandez-Nieves, A.; Stone, H. A.; Weitz, D. A. Dripping to Jetting Transitions in Coflowing Liquid Streams. *Phys. Rev. Lett.* **2007**, *99*, 094502.
- (22) Vanswaay, D.; Tang, T. Y. D.; Mann, S.; DeMello, A. Microfluidic Formation of Membrane-Free Aqueous Coacervate Droplets in Water. *Angew. Chem., Int. Ed.* **2015**, *54*, 8398–8401.
- (23) Eggersdorfer, M. L.; Seybold, H.; Ofner, A.; Weitz, D. A.; Studart, A. R. Wetting Controls of Droplet Formation in Step Emulsification. *Proc. Natl. Acad. Sci. U.S.A.* **2018**, *115*, 9479.
- (24) Abrahamse, A. J.; der Padt, A.; Boom, R. M.; De Heij, W. B. C. Process Fundamentals of Membrane Emulsification: Simulation with CFD. *AIChE J.* **2001**, *47*, 1285–1291.
- (25) Sattari, A.; Hanafizadeh, P. Controlled Preparation of Compound Droplets in a Double Rectangular Co-Flowing Microfluidic Device. *Colloids Surf., A* **2020**, *602*, 125077.
- (26) Priest, C.; Herminghaus, S.; Seemann, R. Generation of Monodisperse Gel Emulsions in a Microfluidic Device. *Appl. Phys. Lett.* **2006**, *88*, 024106.
- (27) Chong, D. T.; Liu, X. S.; Ma, H. J.; Huang, G. Y.; Han, Y. L.; Cui, X. Y.; Yan, J. J.; Xu, F. Advances in Fabricating Double-Emulsion Droplets and Their Biomedical Applications. *Microfluid. Nanofluid.* **2015**, *19*, 1071.
- (28) Thompson, B.; Riche, C. T.; Movsesian, N.; Bhargava, K. C.; Gupta, M.; Malmstadt, N. Engineered Hydrophobicity of Discrete Microfluidic Elements for Double Emulsion Generation. *Microfluid. Nanofluid.* **2016**, *20*, No. 78.
- (29) Liao, C. Y.; Su, Y. C. Formation of Biodegradable Microcapsules Utilizing 3D, Selectively Surface-Modified PDMS Microfluidic Devices. *Biomed. Microdevices* **2010**, *12*, 125.
- (30) Perro, A.; Nicolet, C.; Angly, J.; Lecommandoux, S.; Le Meins, J. F.; Colin, A. Mastering a Double Emulsion in a Simple Co-Flow Microfluidic to Generate Complex Polymersomes. *Langmuir* **2011**, *27*, 9034.
- (31) Huang, S.; Zeng, S.; He, Z.; Lin, B. Water-Actuated Microcapsules Fabricated by Microfluidics. *Lab Chip* **2011**, *11*, 3407–3410.
- (32) Lim, C. N.; Koh, K. S.; Ren, Y.; Chin, J. K.; Shi, Y.; Yan, Y. Analysis of Liquid-Liquid Droplets Fission and Encapsulation in Single/Two Layer Microfluidic Devices Fabricated by Xurographic Method. *Micromachines* **2017**, *8*, 49.
- (33) Partearroyo, M. A.; Ostolaza, H.; Goñi, F. M.; Barberá-Guillem, E. Surfactant-Induced Cell Toxicity and Cell Lysis: A Study Using B16 Melanoma Cells. *Biochem. Pharmacol.* **1990**, *40*, 1323–1328.
- (34) Basu, A. S. Droplet Morphometry and Velocimetry (DMV): A Video Processing Software for Time-Resolved, Label-Free Tracking of Droplet Parameters. *Lab Chip* **2013**, *13*, 1892–1901.
- (35) Kim, C.; Lee, K. S.; Kim, Y. E.; Lee, K. J.; Lee, S. H.; Kim, T. S.; Kang, J. Y. Rapid Exchange of Oil-Phase in Microencapsulation Chip to Enhance Cell Viability. *Lab Chip* **2009**, *9*, 1294.
- (36) Samandari, M.; Alipanah, F.; Javanmard, S. H.; Sanati-Nezhad, A. One-Step Wettability Patterning of PDMS Microchannels for Generation of Monodisperse Alginate Microbeads by in Situ External Gelation in Double Emulsion Microdroplets. *Sens. Actuators, B* **2019**, *291*, 418–425.